

H. Cedar, A. D. Riggs, Eds. (Springer, New York, 1984), pp. 353–378.

4. R. Holliday and J. E. Pugh, *Science* **187**, 226 (1975); A. D. Riggs, *Cytogenet. Cell Genet.* **14**, 9 (1975).
5. E. U. Selker and J. N. Stevens, *Proc. Natl. Acad. Sci. U.S.A.* **82**, 8114 (1985).
6. M. S. Turker, K. Swisshelm, A. C. Smith, G. M. Martin, *J. Biol. Chem.* **264**, 11632 (1989).
7. E. U. Selker, *Trends Biochem. Sci.* **15**, 103 (1990).
8. E. J. Finnegan, R. I. S. Brettell, E. S. Dennis, in (1), pp. 218–261.
9. E. U. Selker, in (1), pp. 212–217; L. Rhounim, J.-L. Rossignol, G. Faugeton, *EMBO J.* **11**, 4451 (1992).
10. D. M. Woodcock, P. J. Crowther, W. P. Diver, *Biochem. Biophys. Res. Commun.* **145**, 888 (1987).
11. M. Toth et al., *J. Mol. Biol.* **214**, 673 (1990).
12. Y. Gruenbaum et al., *Nature* **292**, 860 (1981).
13. E. U. Selker, *Annu. Rev. Genet.* **24**, 579 (1990).
14. H. P. Saluz and J. P. Jost, in (1), pp. 11–26.
15. M. Frommer et al., *Proc. Natl. Acad. Sci. U.S.A.* **89**, 1827 (1992).
16. E. U. Selker and P. W. Garrett, *ibid.* **85**, 6870 (1988).
17. J. H. Kinnaird and J. R. S. Fincham, *Gene* **26**, 253 (1983).
18. J. L. Paluh et al., *Proc. Natl. Acad. Sci. U.S.A.* **85**, 3728 (1988).
19. Segments E and F (Fig. 1) include 105- and 100-bp segments upstream and downstream of the duplicated region, respectively. The amount of methylation detected by genomic sequencing in these two border regions was large (~95% and 99%, respectively), as in the interior regions. Caution must be exercised in drawing quantitative conclusions because of the small number of molecules examined and possible biases in the procedures.
20. B. Margolin and E. Selker, unpublished results.
21. E. U. Selker, B. C. Jensen, G. A. Richardson, *Science* **238**, 48 (1987).
22. W. S. Grayburn and E. U. Selker, *Mol. Cell. Biol.* **9**, 4416 (1989).
23. V. Miao, P. Garrett, E. Selker, unpublished results.
24. E. B. Cambareli, M. J. Singer, E. U. Selker, *Genetics* **127**, 699 (1991).
25. M. Schweizer et al., *Proc. Natl. Acad. Sci. U.S.A.* **78**, 5086 (1981).
26. The *am<sup>FIP-8M</sup>* allele was isolated as a single-copy segregant from a cross of an *am<sup>+</sup>lys1* strain (N261) and a strain (N276) that has the native *am* gene and an ectopic copy of *am* from transformant T-510-5.6 (16).
27. *Neurospora* DNA was isolated from cultures grown 16 hours in supplemented Vogel's minimal medium [1.5% sucrose, lysine (0.6 mg/ml), and alanine (1 mg/ml)] at 33°C with shaking from an inoculum of  $2 \times 10^6$  conidia per milliliter. DNA methylation was prevented in some cultures by including 24  $\mu$ M 5AC initially and adding an equal amount of 5AC after 4 hours. Procedures for DNA isolation and Southern hybridizations were as described (21). The blot was stripped and reprobed for the *qa-2* gene [E. Selker, D. Y. Fritz, M. J. Singer, unpublished results; (25)] to confirm that the digests had gone to completion.
28. We identified mutations by direct sequencing of amplified DNA with primers ~20 bp from the end points of the duplicated region. Amplification was achieved by 28 cycles of PCR (1 min at 50°C, 2 min at 72°C, and 1 min at 94°C) with ~0.5  $\mu$ g of crude genomic DNA in 100  $\mu$ l of reaction buffer (Promega) with 200  $\mu$ M of each nucleotide triphosphate and ~0.5  $\mu$ M of each primer. DNA sequencing was mostly done by cyclic sequencing {Promega *f* mole kit; [<sup>35</sup>S]2'-deoxyadenosine triphosphate (dATP) incorporation method} with a single internal *am* primer and DNA purified from a low-melt agarose gel with Magic PCR Preps (Promega). Our sequencing of the wild-type and mutant *am* alleles revealed four differences relative to the published sequence (17) of this gene. We suggest the following modifications, none of which affect the protein coding region: change C at position 62 to G, add C at position 261,

insert G between positions 2027 and 2028 (ATTG-GTG), and remove G at 2498 (to give a run of only three G's).

29. In preparation for sodium bisulfite modification, 10  $\mu$ g of DNA from *Neurospora am<sup>FIP-8M</sup>* plus 0.4 ng of a 0.3-kb segment of DNA in which 5mC was introduced at every C position were denatured in 235  $\mu$ l of 0.1 M NaOH and 1 mM EDTA at 22°C. After 15 min the solution was neutralized by adding 50  $\mu$ l of 1 M tris-HCl (pH 7.2). The DNA was ethanol precipitated, rinsed, dried, resuspended in 1.2 ml of 3.3 M sodium bisulfite, 0.5 mM hydroquinone (pH 5.0), incubated at 50°C for 23 hours, and dialyzed three times each (2 liters in degassed water; 4°C) against (i) 5 mM sodium acetate (pH 5.2), 0.5 mM hydroquinone, (ii) 0.5 mM sodium acetate (pH 5.2), and (iii) water. The DNA was then concentrated, treated with base, and worked up as described (15) except that the DNA was reprecipitated twice with ammonium acetate and ethanol. PCR reactions (generally 28 cycles of 1 min each at 52°C, 72°C, and 94°C) were carried out on 1  $\mu$ l of modified DNA in 100  $\mu$ l of reaction buffer (Promega) with 200  $\mu$ M of each nucleotide triphosphate, ~0.5  $\mu$ M of each primer (Table 1), and 5 U of Taq DNA polymerase (Promega). Poor yields were obtained when we attempted to amplify fragments larger than ~450 bp from the bisulfite-treated DNA. The product was gel purified with NA45 paper (Schleicher & Schuell), ligated into a "T-vector" (pT7-blue; Novagen), and introduced into DH5 $\alpha$ ' *Escherichia coli* cells by electroporation with a Bio-Rad apparatus and following their protocol. The methylated control template was made by PCR with deoxy-5-methylcytidine triphosphate, deoxyguanosine triphosphate, dATP, and deoxythymidine triphosphate (200  $\mu$ M each) with M13-40 (NEB)

and M13 reverse (U.S. Biochemical) primers and pBluescript SK<sup>+</sup> plasmid (Stratagene) as a template. This template was reamplified from the modified DNA with the same primers. The 98-bp Kpn I-Sac I MCS fragment, which includes 32 C's on one strand and 30 on the other, was isolated and cloned into pDY1, a pBluescript-based plasmid with a readily identifiable insert in the polylinker. The cloned Kpn I-Sac I fragments and the various fragments derived from *Neurospora* DNA were sequenced on both strands with T7 and T3 primers (Stratagene). To test for completeness of the bisulfite modification, we amplified a segment of the *Neurospora cpc1* gene (nucleotides 168 to 481) (18) containing 79 C's on the relevant strand with primers of the following sequences: 5'-GAT-AGGGTGGATTGGTTG and 5'-ACTCATACTTC-CCCCTTTRRC. Sequencing of both unmethylated and methylated control templates was done for each batch of bisulfite-treated DNA. Several regions of *am<sup>FIP-8M</sup>* allele were sequenced with more than one batch of bisulfite-treated DNA, but all data presented came from a single reaction.

30. We thank M. Frommer for communications to us before publication about the bisulfite genomic sequencing method and M. Crabtree for help with some of the DNA sequencing. We also gratefully acknowledge B. Margolin and A. Selker for help organizing some of the data and A. Bird for hospitality to E.U.S. during sabbatical. We thank F. Antequera, A. Bird, and members of our laboratory for comments on the manuscript. Supported by NIH grant GM 35690 and NSF grant DCB 8718163. This work was done during the tenure of an Established Investigatorship of the American Heart Association.

21 July 1993; accepted 28 October 1993

## Initiation at Closely Spaced Replication Origins in a Yeast Chromosome

Bonita J. Brewer\* and Walton L. Fangman

Replication of eukaryotic chromosomes involves initiation at origins spaced an average of 50 to 100 kilobase pairs. In yeast, potential origins can be recognized as autonomous replication sequences (ARSs) that allow maintenance of plasmids. However, there are more ARS elements than active chromosomal origins. The possibility was examined that close spacing of ARSs can lead to inactive origins. Two ARSs located 6.5 kilobase pairs apart can indeed interfere with each other. Replication is initiated from one or the other ARS with equal probability, but rarely (<5%) from both ARSs on the same DNA molecule.

Eukaryotic origins of replication are activated at different times during the period of DNA replication of the cell cycle (S phase). DNA fiber autoradiography experiments have suggested that adjacent origins are activated at about the same time (1, 2). Such experiments do not examine specific origins, and they only detect adjacent origins when both are active in the same S phase. As part of a study of the temporal regulation of origin activation, we previously inserted *ARS1*, an origin activated early in S phase, next to a late activated origin, *ARS501*, located about 30 kb from a telomere. The *ARS1* sequences are late repli-

cating in this new context (3). Using two-dimensional (2D) agarose gel electrophoresis, we analyzed the replication of this region to assess the level of origin activity at each ARS.

Three yeast strains were used in this study. They are isogenic except for the ARS content on the right arm of chromosome V. RM14-3a (4) has the normal chromosome structure, which includes *ARS501*, a single-copy origin approximately 30 kb from the telomere (Fig. 1). The 1.45-kb Eco RI *TRP1ARS1* fragment has been inserted at the Eco RI site, 6 kb telomere proximal to *ARS501*, to create the second strain, BF14-3a::*ARS1* (3), which now contains two ARSs, 6.5 kb apart. This strain was used to create a third strain in which *ARS501* was deleted by replacement of the *Sna* BI-Xho I ARS fragment with *URA3*

Department of Genetics SK-50, University of Washington, Seattle, WA 98195.

\*To whom correspondence should be addressed.

(designated BB14-3a::ARS1/ARS501Δ). The closest flanking origins lie more than 40 kb toward the centromere and more than 21 kb toward the telomere (5).

If a restriction fragment has an active origin near its center, then during replication the two forks moving out from the origin will first give rise to a series of bubbles, and later to a series of large simple Y's when one of the forks passes the nearest restriction site (6) (Fig. 2A). When the Msc I fragment that spans the new ARS1 in strain BF14-3a::ARS1 was examined on a 2D gel, a bubble pattern with large simple Y's was found (Fig. 2B), indicating that ARS1 is active as an origin at this new location. However, the arc of replication intermediates that emerges from the spot containing nonreplicating linear molecules include both bubbles and small simple Y's. These small simple Y's may be the consequence of replication initiating outside the Msc I fragment—initiating at ARS501, for example, but not at ARS1. Alternatively, the small simple Y's may result from breakage of bubbles in vitro. If the former explanation were correct, then deletion of ARS501 should reduce the number of simple Y's arising from the Msc I linears. Analysis of the identical Msc I fragment from the ARS501 deletion chromosome (Fig. 2C) reveals that the initial part of the ARS1 simple Y arc is diminished relative to the bubble arc. The remaining small simple Y's are likely to result from breakage. We conclude that ARS1 is active in this ectopic location, but that the efficiency of activation is influenced by the presence of the native origin, ARS501, 6.5 kb away.

To determine whether this interaction is reciprocal, we examined the Xba I fragment containing ARS501 on 2D gels. In its normal context, ARS501 is an efficiently activated origin (5) (Fig. 2D). Insertion of ARS1 (Fig. 2E) augments ARS501's simple Y arc and diminishes its bubble arc. Thus, just as ARS1's activation efficiency on chromosome V is decreased by the presence of ARS501 (Fig. 2, B and C), ARS501's activation efficiency is decreased by the presence of ARS1 nearby (Fig. 2, D and E).

We then investigated whether the two neighboring origins were ever active on the same chromosome. If both origins were used simultaneously, then the fragment that lies between the two potential origins would be replicated by forks that enter from both ends and meet within the fragment. These replication intermediates will have shapes (double Y or H forms) that are distinguishable on 2D gels from both simple Y's and bubbles (6) (Fig. 3A). The majority of replication intermediates for the Eco RI fragment (Fig. 3, B and C) and an adjacent overlapping fragment (7) are simple Y's from both strains: double Y intermediates

are rare. We estimate that simultaneous activation of both ARS1 and ARS501 occurs in fewer than 5% of the chromosomes V. We conclude that there is an apparent interference between adjacent, closely spaced origins. Perhaps initiation at the two origins is temporally staggered by more time than it takes for forks initiated at one origin to reach the other. With an estimated replication fork progression rate of 3.7 kb/min (2), activation of these two nearby origins would have to differ by more than 2 min to eliminate the double Y's. Alternatively, there might be a direct interference between adjacent origins. This interference might be topological—with interference transmitted through the DNA itself—or there may be a local competition for limiting initiation factors.

Given that either ARS1 or ARS501 is activated to replicate the domain at the right arm of chromosome V, we wished to deter-

mine the relative contributions of the two origins. The ratio of bubbles to simple Y's in the 2D gels (Fig. 2) does not provide a reliable estimate of origin use because of fork breakage in vitro. However, an estimate of origin efficiency can be obtained by determining the direction in which forks move through restriction fragments that flank the origins. Direction of fork movement is deduced by examining the replication intermediates of a fragment from which one end has been truncated by a second restriction digestion after the first dimension of gel electrophoresis (8, 9) (Fig. 4A). If the fork exits the fragment at the end that is removed by the second digestion, then the simple Y intermediates arise from the spot of unbranched restriction fragments (dashed arc, Fig. 4A). If the fork enters the fragment at the end that is removed, then the simple Y intermediates are displaced from this spot of linears (solid arc, Fig. 4A).

**Fig. 1.** Map of the ARS501 region of chromosome V in yeast strain RM14-3a. The telomere (TEL) is to the right, the centromere (CEN) is to the left. Positions of ARS's are indicated by vertical arrows, and positions of genes *DMC1* (15), *TRP1*, and *URA3* are indicated by horizontal arrows. Only restriction sites pertinent to this study are shown. Below the map, and connected to it by dashed lines, are the two alterations made to the wild-type chromosome. To create strain BF14-3a::ARS1, the 1.45-kb *TRP1*ARS1 fragment from chromosome IV was inserted at the indicated Eco RI site. To create strain BB14-3a::ARS1/ARS501Δ, ARS501 was replaced by the *URA3* gene. Bar represents 2 kilobase pairs. Sn, Sna BI; Xh, Xho I; Xb, Xba I; E, Eco RI; EV, Eco RV M; Msc I; P, Pst I; and Sp, Spe I.

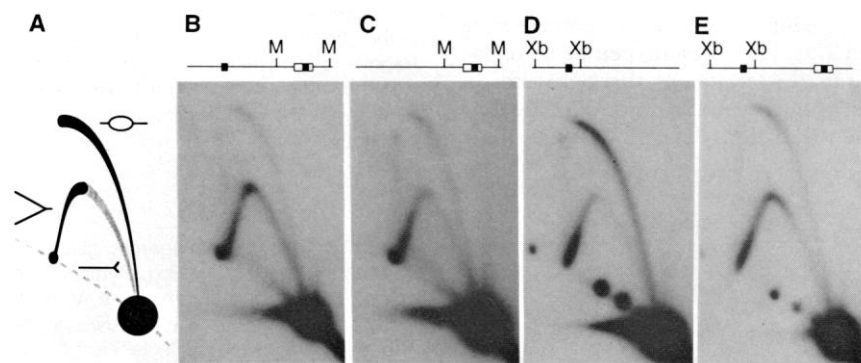
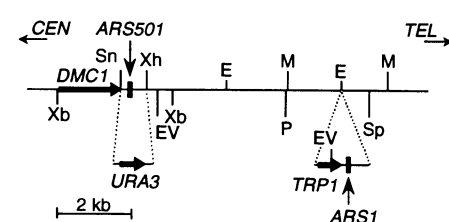


**Fig. 2.** Two-dimensional agarose gels of ARS1 and ARS501. (A) Patterns expected for bubble and simple Y replication intermediates (6). (B and C) The 3.8-kb Msc I fragment from chromosome V that contains the integrated copy of ARS1 was detected on 2D gels by hybridization to the Msc I fragment cloned from RM14-3a. (B) Strain BF14-3a::ARS1. (C) Strain BB14-3a::ARS1/ARS501Δ. (D and E) The 3.1-kb Xba I fragment from chromosome V that contains ARS501 was detected on 2D gels by hybridization to the cloned fragment. (D) Strain RM14-3a. (E) Strain BF14-3a::ARS1. The cartoons above each panel (B through E) illustrate the ARS composition of the chromosomes being studied. The solid black box represents an ARS (either ARS1 or ARS501), the open rectangle is the 1.45-kb *TRP1*ARS1 insert. DNA was isolated (9, 16) from pooled S-phase culture samples after the *MATa cdc7* cells were synchronized with sequential incubations in  $\alpha$ -factor and at 37°C. Nuclear DNA (3 to 5  $\mu$ g) was digested with the appropriate enzyme for 5 hours and then subjected to electrophoresis, first (from left to right) in a 0.4% tris-borate EDTA (TBE)-agarose gel at 1 V/cm for 20 hours, and second (from top to bottom) in a 1.1% TBE-agarose gel with ethidium bromide (0.3  $\mu$ g/ml) at 5 to 6 V/cm for 5 to 6 hours at 4°C. Blotting and hybridization were as described (6). Additional spots on the arc of linears result from partial digestion or cross-hybridizing chromosomal fragments.

The Eco RV fragment between *ARS501* and *ARS1* was examined by a 2D gel in which *in situ* digestion by Pst I was carried out. As controls, the two single-ARS strains were also examined either as an Eco RV-Spe I fragment (RM14-3a) or as an Eco RV fragment (BB14-3a::*ARS1/ARS501Δ*). In the normal chromosome, with only *ARS501* present, the arc of replication intermediates arises from the monomer spot (Fig. 4B), indicating that forks are moving away from *ARS501* toward the telomere. In contrast, in the strain that has only the *ARS1* insert (BB14-3a::*ARS1/ARS501Δ*), the arc of simple Y's is not continuous with the monomer spot but is displaced horizontally (Fig. 4D), indicating that forks move in the opposite direction (away from *ARS1* toward the centromere). When the same fragment from the strain with *ARS1* integrated next to *ARS501* is examined, the 2D gel pattern is a composite of the two patterns seen for the intermediates from the single ARS chromosomes (Fig. 4C). These results indicate that in some cells the replication fork is moving toward the telomere from *ARS501*, whereas in other cells the replication fork is moving toward the centromere from *ARS1*. From the relative intensities of the two arcs we estimate that these two ARSs are equally efficient in initiation.

Finally, we examined the direction of fork movement in the regions flanking *ARS501* and *ARS1* in all three strains. In fragments on the telomere side of *ARS1*, only forks moving toward the telomere were found (7). Similarly, in a fragment on the centromere side of *ARS501*, only forks moving toward the centromere were found (7). These results permit us to say that, in this region of the right arm of chromosome V, *ARS501* or *ARS1* are used in the vast majority of cells—that is, these

are efficient origins of replication. But when the two origins are within 6.5 kb of each other, either *ARS1* only or *ARS501* only serves as the origin for this late-replicating domain. It is a rare occurrence (<5%) for both origins to be active on the same chromosomal DNA molecule. Whether this origin interference is the consequence of direct origin-origin interference or the consequence of asynchrony in the activation of adjacent origins will require further study.

The average spacing between active origins in yeast chromosomes has been measured by both electron microscopy (10) and DNA fiber autoradiography (2)

and was found to be between 35 and 90 kb, with individual values ranging from 3 kb to more than 150 kb. To date, the leftmost two-thirds of chromosome III is the largest yeast contig in which both ARSs and origins have been systematically mapped (11). The 14 ARSs have an average spacing of 15 kb (ranging from ~1 to 45 kb), and the five efficient origins are spaced an average of 38 kb apart (ranging from 20 to 45 kb). *ARS308* is an inefficient origin on chromosome III (12) and also functions poorly in the ARS plasmid assay (13). In its native position on chromosome III, *ARS308* resides approximately 7 kb from an efficient origin, *ARS307*.

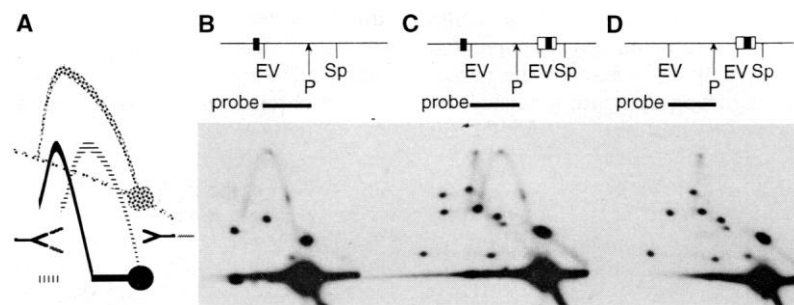


**Fig. 4.** Determining the direction of fork movement between two ARSs. (A) Pattern expected for a fragment that is replicated by a single fork moving in either direction. The uppermost arc represents the simple Y pattern that the fragment would display in a normal 2D gel. The patterns below result from cleavage of the fragment (at a site one-third of the distance into the fragment from the right end) after the first dimension of electrophoresis. The truncated fragments migrate faster through the gel, relative to the uncut fragments. The replication intermediates arise from the spot containing linears (dashed arc) if the fork had been moving to the right through the fragment, but are displaced from the spot of linears (solid arc) if the fork had been moving to the left. [See (8) and (9) for a more complete discussion of the technique and its interpretations.] (B) The Eco RV-Spe I fragment from strain RM14-3a cut *in situ* with Pst I was detected with a cloned probe from the Eco RV-Pst I portion of the chromosome. The additional spots represent cross-hybridization to other chromosomal DNA fragments. (C) The Eco RV fragment from strain BF14-3a::*ARS1* cut *in situ* with Pst I and hybridized with the same probe as in (B). (D) The Eco RV fragment from strain BB14-3a::*ARS1/ARS501Δ* cut *in situ* with Pst I and hybridized with the same probe as in (B). Chromosomes are diagrammed above (B through D). The solid black boxes represent ARSs, the open rectangle is the *TRP1ARS1* insert.

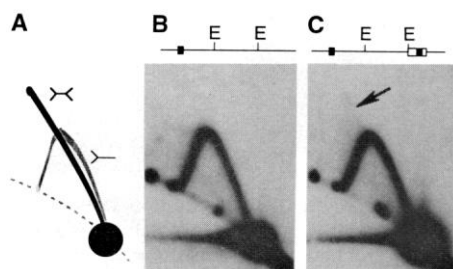
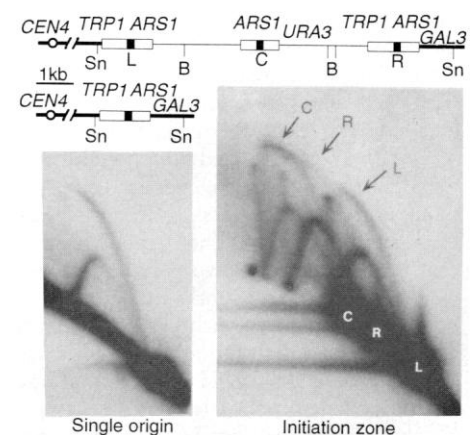


**Fig. 3.** Two-dimensional agarose gels of the potential replication terminus between *ARS1* and *ARS501*. (A) Pattern expected for double Y's (6). The 3.1-kb Eco RI fragment from strains RM14-3a (B) and BF14-3a::*ARS1* (C) were detected by a probe from the cloned fragment. The chromosomes are diagrammed above (B and C). The solid black boxes represent ARSs, the open rectangle is the *TRP1ARS1* insert. Electrophoresis and hybridization are as described in Fig. 2. The rare double Y intermediates are indicated by the arrow.

**Fig. 5.** Two-dimensional agarose gels of single and tandem copies of *ARS1*. Partial restriction maps of a modified chromosome IV (top) and the wild-type chromosome IV are diagrammed. The three copies of *ARS1*, labeled L (left), C (center), and R (right), are separated by pBR322 vector sequences and the *URA3* gene (thin line). The left autoradiogram shows the bubble and simple Y arcs for the single *ARS1* fragment (2.5 kb) in the wild-type chromosome, detected by the 1.45-kb Eco RI *TRP1ARS1* probe. The right autoradiogram shows the replication intermediates for the three *ARS1* fragments in the modified chromosome (L, 2.5 kb; C, 4.3 kb; R, 3.3 kb), detected by the same probe. The arrows point to the bubble arcs arising from each of the three *ARS1*-restriction fragments. By comparing the intensity of the bubble arcs relative to the simple Y arcs it appears that none of the three copies of *ARS1* in this initiation zone is as efficiently used as the single *ARS1* in the wild-type chromosome. In addition, the three copies of *ARS1* differ in their efficiency of activation—of the three potential origins in the initiation zone, replication begins most often at *ARS1*-C and least often at *ARS1*-R.



When ARS307 is deleted from the chromosome, ARS308 continues to be an inefficient origin; it does not take over the replication initiation function for this region of the chromosome (12). In this case, close spacing is clearly not the explanation for inactivation of ARS308. It is more likely that ARS308 lacks sequence elements that are required for efficient initiation. It is not known over what distance efficient origins exert their interference. Nor is it known whether there might be a threshold distance for origin interference or a gradual increase in interference as origins are brought into closer proximity.

We speculate that if we were to add a third or a fourth ARS in close proximity to ARS1 and ARS501, we would see further diminution of initiation at each of the ARSs. Consequently, there would be an increase in the number of replication forks passing through each ARS because of initiation at one of the flanking origins. In this region each restriction fragment that contains an ARS near its center would give the same 2D gel pattern—that is, a faint bubble arc with a very prominent complete simple Y arc. Two additional copies of ARS1 have been integrated 3.5 kb apart at the normal locus of ARS1 on chromosome IV (Fig. 5). It appears that the three copies of ARS1 share the responsibility of initiating replication in this chromosomal region: simultaneous activations of adjacent origins are rare, and each copy of ARS1 displays a faint bubble arc and a more prominent arc of simple Y's on 2D gels (Fig. 5). When overlapping fragments from the 55-kb initiation zone of the amplified DHFR locus of Chinese hamster ovary cells are examined on 2D gels (14), each fragment gives this composite pattern. It has been suggested that a broad initiation zone reflects the lack of specific origin sequences. However, we conclude that the data from the DHFR locus are also consistent with the close spacing of multiple, specific initiation sites that experience origin interference.

## REFERENCES AND NOTES

- J. A. Huberman and A. D. Riggs, *J. Mol. Biol.* **32**, 327 (1968).
- C. J. Rivin and W. L. Fangman, *J. Cell Biol.* **85**, 108 (1980).
- B. M. Ferguson and W. L. Fangman, *Cell* **68**, 333 (1992).
- R. M. McCarroll and W. L. Fangman, *ibid.* **54**, 505 (1988).
- B. M. Ferguson, B. J. Brewer, A. E. Reynolds, W. L. Fangman, *ibid.* **65**, 507 (1991).
- B. J. Brewer and W. L. Fangman, *ibid.* **51**, 463 (1987).
- \_\_\_\_\_, unpublished results.
- W. L. Fangman and B. J. Brewer, *Annu. Rev. Cell Biol.* **7**, 375 (1991).
- B. J. Brewer, D. Lockson, W. L. Fangman, *Cell* **71**, 267 (1992).
- C. S. Newlon and W. Burke, *ICN-UCLA Symp. Mol. Cell. Biol.* **19**, 211 (1980).
- C. S. Newlon *et al.*, *Genetics* **129**, 343 (1991).
- S. A. Greenfeder and C. S. Newlon, *Mol. Biol. Cell* **3**, 999 (1992).
- L. Clarke and J. Carbon, *Nature* **287**, 504 (1980).
- J. L. Hamlin, *Bioessays* **14**, 651 (1992).
- D. K. Bishop, D. Park, X. Liuzhong, N. Kelckner, *Cell* **69**, 439 (1992).
- J. A. Huberman *et al.*, *ibid.* **51**, 473 (1987).
- We thank J. Diller, K. Friedman, K. Kolor, D. Lockshon, and M. K. Raghuraman for comments on the manuscript. Supported by the National Institute of General Medical Sciences grant 18926 (to B.J.B. and W.L.F.).

22 June 1993; accepted 31 August 1993

## Association of the APC Gene Product with $\beta$ -Catenin

Bonnee Rubinfeld, Brian Souza, Iris Albert, Oliver Müller, Scott H. Chamberlain, Frank R. Masiarz, Susan Munemitsu, Paul Polakis\*

Mutations in the human APC gene are linked to familial adenomatous polyposis and to the progression of sporadic colorectal and gastric tumors. To gain insight into APC function, APC-associated proteins were identified by immunoprecipitation experiments. Antibodies to APC precipitated a 95-kilodalton protein that was purified and identified by sequencing as  $\beta$ -catenin, a protein that binds to the cell adhesion molecule E-cadherin. An antibody specific to  $\beta$ -catenin also recognized the 95-kilodalton protein in the immunoprecipitates. These results suggest that APC is involved in cell adhesion.

Multiple genetic alterations, including mutations in RAS and in the tumor suppressor genes APC, P53, and DCC, contribute to the progression of colorectal tumorigenesis [reviewed in (1)]. Among these, APC mutations appear earliest in the pathway and are observed in small benign adenomas of the colon (2). Mutations in APC are also linked to an inherited form of colon cancer, familial adenomatous polyposis (3, 4). The protein product of APC is a 2844-amino acid polypeptide containing a potential coiled-coil structure in the NH<sub>2</sub>-terminal region, a repeated 20-amino acid sequence in the central region, and a stretch of basic amino acids in the COOH-terminal region (3). The APC mutations associated with cancer result in the production of APC proteins that are truncated at the COOH-terminus (2, 5, 6). How these deletions compromise APC function is unknown, as no functions have yet been ascribed to the protein, except for the homo-oligomerization domain localized to the extreme NH<sub>2</sub>-terminus (7).

To characterize the APC protein, we generated polyclonal antisera against two separate regions of the polypeptide. One antiserum, anti-APC2, recognized epitopes in the central region of the protein, and the other, anti-APC3, was specific to the

COOH-terminal region (Fig. 1A). The antibodies were tested on the colorectal cancer cell lines SW480, HCT116, and DLD-1, and the kidney cell line 293 (8). Anti-APC2 reacted with the full-length, wild-type APC from 293 cells and with mutant APC from SW480 cells (Fig. 1B). Full-length APC was immunoprecipitated from the 293 and the HCT116 cells by both anti-APC2 and anti-APC3. By contrast, only anti-APC2 recognized the mutant APC in the SW480 and DLD-1 cells. The single APC allele in the SW480 cells contains a nonsense mutation at codon 1338 (9) and produces a stable truncated form of APC (6). The DLD-1 cells also express a mutant APC similar in size to that detected in SW480 cells (Fig. 1B).

To identify proteins potentially associated with APC, we performed immunoprecipitations on lysates from cells metabolically labeled with [<sup>35</sup>S]methionine. The antibodies to APC immunoprecipitated wild-type APC from the 293 and HCT116 cell lysates, but only the truncated APC from the SW480 cells (Fig. 2A). In addition to APC, a prominent radiolabeled protein of ~95 kD was present in anti-APC2 immunocomplexes from HCT116, 293, and SW480 cells. The 95-kD protein was also detected in anti-APC3 immunoprecipitates from HCT116 and 293 cells, but not from SW480 cells. This result demonstrated that the 95-kD protein is associated with APC and does not react directly with the antibodies to APC. Other polypeptides were also immunoprecipitated by antibodies to APC; however, most of these proteins appeared to bind nonspecifically.

B. Rubinfeld, B. Souza, I. Albert, O. Müller, S. Munemitsu, P. Polakis, Onyx Pharmaceuticals, 3031 Research Drive, Richmond, CA 94806.  
S. H. Chamberlain, Protein Chemistry Section, Chiron Corporation, 4650 Horton Street, Emeryville, CA 94608.  
F. R. Masiarz, Protein Chemistry Section, Chiron Corporation, and University of California, San Francisco, CA 94143.

\*To whom correspondence should be addressed.